CHEMISTRY
A EUROPEAN JOURNAL

DOI: 10.1002/chem.200501527

Preparation of Highly Conductive, Self-Assembled Gold/Polyaniline Nanocables and Polyaniline Nanotubes

Kun Huang,[a] Yuanjian Zhang,[a] Yunze Long,[b] Junhua Yuan,[a] Dongxue Han,[a] Zhijuan Wang,[a] Li Niu,*[a] and Zhaojia Chen*[b]

Abstract: One-dimensional gold/polyaniline (Au/PANI-CSA) coaxial nanocables with an average diameter of 50–60 nm and lengths of more than 1 μm were successfully synthesized by reacting aniline monomer with chlorauric acid ($HAuCl_4$) through a self-assembly process in the presence of D-camphor-10-sulfonic acid (CSA), which acts as both a dopant and surfactant. It was found that the formation probability and the size of the Au/PANI-CSA nanocables depends on the molar ratio of aniline to $HAuCl_4$ and the concentration of CSA, respectively. A synergistic growth mechanism was proposed to interpret the formation of the Au/PANI-CSA nanocables. The directly measured conductivity of a single gold/polyaniline nanocable was found to be high ($\approx 77.2\ S\,cm^{-1}$). Hollow PANI-CSA nanotubes, with an average diameter of 50–60 nm, were also obtained successfully by dissolving the Au nanowire core of the Au/PANI-CSA nanocables.

Keywords: conducting materials · nanocables · nanotubes · polyaniline · self-assembly

Introduction

Coaxial nanocables as a new type of one-dimensional (1D) nanostructure have attracted considerable attention in recent years due to their potential application in gated field-effect transistors, quantum wire lasers, and nanoscale electronic devices.[1,2] Several solution-based template and template-free methods have been demonstrated to generate polymer/polymer, semiconductor/polymer, and metal/polymer nanocables at relatively low temperatures. For instance, many 1D nanomaterials (such as, Au,[3] Ag,[4] Ni,[5] carbon nanotubes (CNTs),[6] etc.) are often used as templates to prepare the nanocables. In this method, the surface of the nanowires are coated with conformal sheaths made of different materials by chemical, electrochemical, sol–gel, or other routes, to form coaxial nanocables. In addition, some mesoporous silica materials[7] and peptides[8] can also act as templates to prepare such 1D nanocables, in which their hollow structures can be filled with metals and other functional materials. More recently, Yu et al. have reported the synthesis of Ag/carbon and Ag/cross-linked poly(vinyl alcohol) coaxial nanocables through a hydrothermal coreduction process in the absence of a template.[9]

Currently, there is considerable interest in 1D conducting polymer nanostructures because of their unique properties and promising potential applications in nanodevices, such as, nanowires,[10,11] sensor/actuator arrays,[12,13] and optoelectric devices,[14,15] as well as in biotechnology[16,17] (e.g., delivery agents, pharmaceutical agents). In particular, coaxial nanostructures, containing metal or inorganic electrical, optical, and magnetic nanorods/nanowires coated with conducting polymers, provide an exciting system with which to investigate the possibility of designing device functionality, because the core–shell structure of nanocables often exhibits different chemical and physical properties from those of the sole core or shell materials. Recently, conducting polymer coaxial nanocables have been reported in the literature. Xu et al.,[18] for instance, reported the template synthesis and magnetic behavior of an array of cobalt nanowires encapsulated in polyaniline nanotubules, in which the polyaniline envelope protected the metal nanowires from oxidation and corro-

[a] Dr. K. Huang, Y. Zhang, J. Yuan, D. Han, Z. Wang, Prof. Dr. L. Niu
State Key Laboratory of Electroanalytical Chemistry
Changchun Institute of Applied Chemistry
Graduate School of the Chinese Academy of Sciences
Chinese Academy of Sciences, Changchun 130022 (China)
Fax: (+86) 431-526-2800
E-mail: lniu@ciac.jl.cn

[b] Dr. Y. Long, Prof. Dr. Z. Chen
Laboratory of Extreme Condition Physics
Institute of Physics
Chinese Academy of Sciences, Beijing, 100080 (China)
Fax: (+86) 431-526-2800
E-mail: zjchen@aphy.iphy.ac.cn

sion, making them stable in air. Kim et al.[19] synthesized Au/polypyrrole core–shell nanorods with Au nanorods as the template. Shi et al.[20] have also reported the electrochemical fabrication of polythiophene-film-coated metallic nanowire arrays. Li et al.[21] fabricated Ag/polypyrrole coaxial nanocables through a one-step process. Recently, Yang et al. also reported that polyaniline nanofibers decorated with Au nanoparticles exhibited nonvolatile memory behavior.[22] Despite many of these studies on the preparation of conducting metal–polymer nanocables, no paper dealing with the preparation and properties of gold/polyaniline nanocables has been published yet.

In this article, the synthesis and characterization of novel gold/polyaniline (Au/PANI) coaxial nanocables synthesized through a self-assembly process in the presence of chlorauric acid ($HAuCl_4$) as the oxidant and D-camphor-10-sulfonic acid (CSA) as the dopant are reported for the first time. The hydrophilic $-SO_3H$ group of CSA acts as both a dopant and surfactant at the same time; when functioning as a dopant this results in electrical properties in the polyaniline layer, whereas as a surfactant it acts as a soft template in the formation of the nanocables. The resulting single nanocables of Au/PANI show high conductivity ($\approx 77.2\ S\,cm^{-1}$). The influence of the synthesis conditions on the morphology, size, and electrical properties of the Au/PANI-CSA nanocables was investigated, and their formation mechanism is discussed.

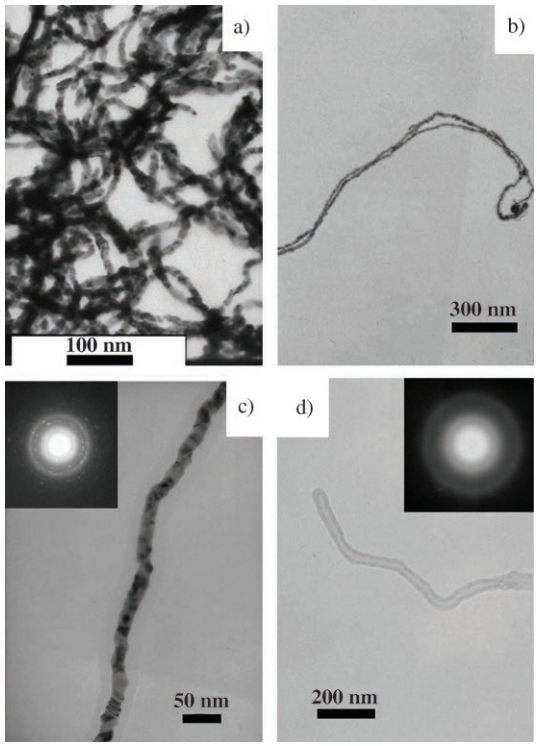

Figure 1. TEM images of the Au/PANI-CSA nanocables and the hollow PANI-CSA nanotubes obtained by dissolving their gold cores in an I_2/KI solution: a) and b) the Au/PANI-CSA nanocables at low magnification; c) the Au/PANI-CSA nanocables at high magnification (inset: an ED pattern of the Au/PANI-CSA nanocables); d) the hollow PANI-CSA nanotubes at low magnification (inset: an ED pattern of the hollow PANI-CSA nanotubes).

Results and Discussion

Morphology and formation mechanism: Figure 1a and b are representative transmission electron microscopy (TEM) images of the sample at low magnification showing that the as-prepared nanocables are 50–60 nm in diameter and more than 1 μm in length. A typical TEM image of the nanocables at higher magnification is shown in Figure 1c, from which it can be seen that the Au/PANI-CSA composites are coaxial nanocable structures composed of PANI-CSA sheaths and gold nanowire cores. The outer diameter of the nanocables is 50–60 nm and the diameter of the central gold cores is 20 nm. Moreover, Figure 1c clearly demonstrates a sharp contrast between the surrounding light polymer and the inner, dark gold cores. An electron diffraction (ED) pattern (inset in Figure 1c) of this area shows the diffraction dots of gold and the characteristic rings of polymer, which further proved that the composite consists of amorphous PANI-CSA polymer with an encapsulated gold nanowire core.

It is known that gold can be easily oxidized into Au^{3+} ions in a saturated I_2 solution. Therefore, a simple experiment was carried out to leach out the Au nanowire cores using I_2. The Au/PANI-CSA nanocables were kept in the iodine solution for more than 5 h, and then they were centrifuged to isolate the precipitate that contained the PANI-CSA hollow nanotubes. The hollow tubule structures of PANI-CSA can be clearly observed in the TEM image shown in Figure 1d. The diameter of the outer shell and the central hollow cores of the PANI-CSA nanotubules are 50–60 and 20 nm, respectively, which are consistent with the above-mentioned nanocable values (as shown in Figure 1c). The ED pattern (inset in Figure 1d) does not display Au diffraction dots or circles confirming that the gold nanowire cores were dissolved completely and that the nanotubes are only amorphous PANI-CSA polymer.

To elucidate the formation mechanism of the Au/PANI-CSA nanocables, the influence of the synthesis conditions (such as, the reaction temperature, the concentration of reactants, and polymerization time) on the morphology and size of the resulting nanostructures was investigated. In this method, it was found that the molar ratio of aniline (An) to $HAuCl_4$ and the concentration of dopant CSA have significant effects on the formation of Au/PANI-CSA nanocables. Figure 2 shows a typical example of the effect of the [An]/[$HAuCl_4$] ratio on the morphology, measured by using TEM. When the [An]/[$HAuCl_4$] ratio was 25:1, irregular polyaniline grains were observed (Figure 2a,b) in which only small gold nanoparticles were embedded in the polyaniline matrix. Interestingly, and in a sharp contrast to the previous result, regular Au/PANI-CSA nanocables with diameters of 50–60 nm and lengths of 1–2 μm became dominant when the [An]/[$HAuCl_4$] ratio was 7:1, as shown in Figure 1a,b. Once the [An]/[$HAuCl_4$] ratio was decreased to 1:1, however, ir-

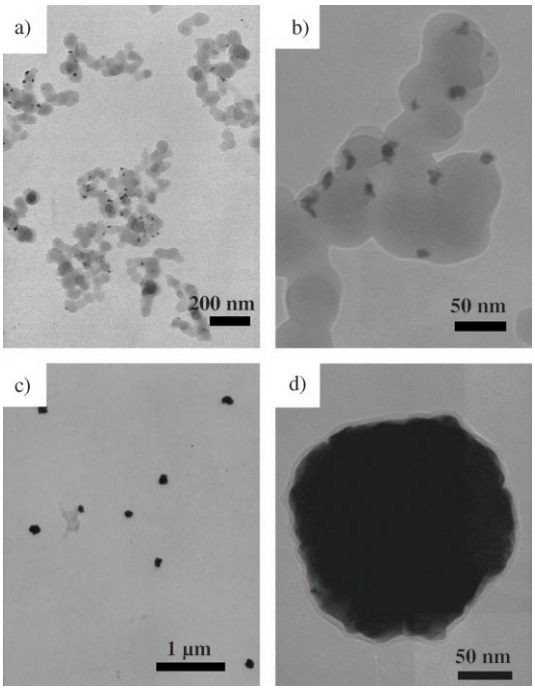

Figure 2. Influence of the molar ratio of aniline to $HAuCl_4$ on the morphology of Au/PANI-CSA: a) and b) 25:1; c) and d) 1:1 (other reaction conditions: [An] = 0.07 M, [CSA] = 0.07 M, reaction time = 10 h, T = 0–5 °C).

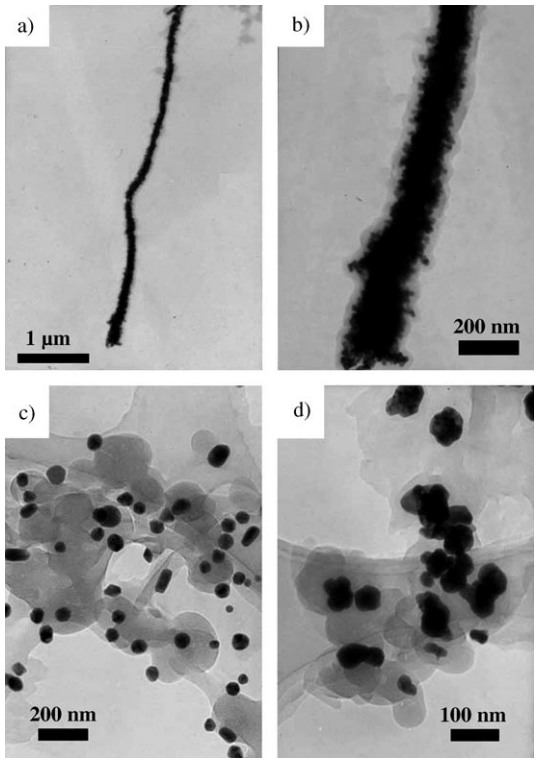

Figure 3. Influence of the concentration of CSA on the morphology of Au/PANI-CSA: a) and b) 0.35 M; c) and d) 0.01 M (other reaction conditions: [An] = 0.07 M, [$HAuCl_4$] = 0.05 M, reaction time = 10 h, T = 0–5 °C).

regular gold grains appeared (Figure 2c,d). The enlarged view shows that the gold grains were coated by a thin layer of polymer. These results indicate that for Au/PANI-CSA a change in morphology of PANI grains to Au/PANI-CSA nanocables to gold grains took place when the [An]/[$HAuCl_4$] ratio changed from 25:1 to 7:1 to 1:1. We also observed that the concentration of CSA affected the size of the nanocables. Au/ANI-CSA nanocables with larger diameters (180 nm) and longer lengths (1–5 μm) were obtained, for example, when a higher concentration of CSA was used (Figure 3a,b). Therefore, it was possible to control the diameter and length of the nanocables by changing the concentration of the dopant. However, if a lower concentration of CSA was used, no such cables were obtained (Figure 3c,d).

The present method of synthesizing Au/PANI-CSA nanocables is similar to other routes with the exception of using different oxidants or dopants. However, the products described here possess a unique coaxial nanocable structure, which is much different from the previously reported morphologies (such as, Au/polyaniline nanoparticles, polyaniline nanofibers and nanobelts).[23–26] Although the formation mechanism of the Au/PANI-CSA nanocables is not fully clear at this stage, the above-mentioned results allow us to suggest a possible process responsible for the formation of such unusual nanocables. We propose that the formation of such Au/PANI-CSA coaxial nanocables is controlled by a synergistic growth mechanism (shown in Scheme 1). First, aniline easily reacts with CSA to form a protonated aniline/CSA salt through a base/acid reaction. When the protonated

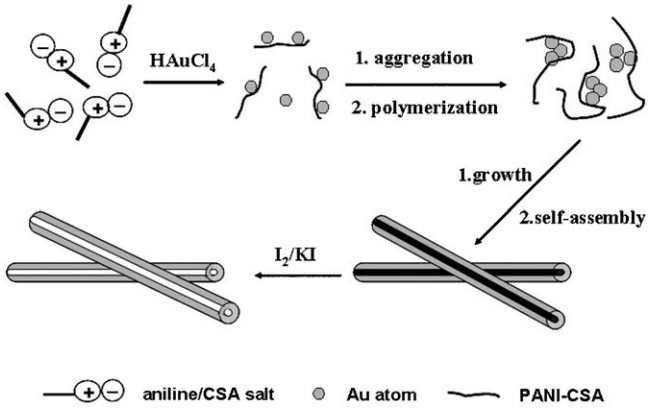

Scheme 1. Illustration of the proposed formation mechanism of Au/PANI-CSA nanocables.

anilinium cations are mixed with the chloroaurate acid, the reduction of $HAuCl_4$ and oxidation of aniline occur simultaneously, leading to the formation of gold nanoclusters and aniline oligomers. Second, in this system, the dopant CSA plays an important role both in the formation of Au/PANI-CSA nanocables and in the further directed growth of gold nanowires capped by the PANI-CSA oligomers or CSA dopant. In fact, CSA has both a doping and surfactant function due to its hydrophilic $-SO_3H$ group. Therefore, it is expected that micelles formed by CSA, or by anilinium cations

might act as soft templates in the formation of the Au/PANI-CSA nanocables. Furthermore, in turn, the gold nanowires act as a backbone on which the PANI-CSA shells can form through a self-assembly process. Finally, the gold nanowire cores can be dissolved by a saturated I_2 solution to form the PANI-CSA nanotubes.

Structural characterization of the Au/PANI-CSA nanocables: Figure 4 shows the UV-visible spectra recorded from the reaction mixture at different reaction stages. The reactant aniline in aqueous CSA solution has an absorbance band centered at $\lambda = 260$ nm (as shown in curve a of Figure 4) that is associated with the characteristic π–π* transition of a benzene ring. Upon introduction of $HAuCl_4$, the solution changed from colorless to red–brown. The time-dependent changes of the reaction mixture are presented in curves b ($t = 0.5$ h) and c ($t = 10$ h) of Figure 4. When the reaction time is about 0.5 h, three new absorbance bands appear at $\lambda = 443$, 530, and 730 nm (Figure 4b). The bands at $\lambda = 443$ and 730 nm are assigned to the characteristic π–π* and localized polaron–π transitions of the emeraldine form of PANI oligomers,[27] which confirms that PANI is formed in the solution. However, the absorption peak at $\lambda = 530$ nm is related to the surface plasmon resonance band of the Au nanoparticles. This means Au nanoparticles were formed in the solution.[28] Significant changes in the absorbance bands are observed in curve c after a reaction time of 10 h. The absorbance bands at $\lambda = 443$ and 730 nm disappear. This behavior suggests that the precipitation of the PANI composites from solution takes place because the chain length of the PANI oligomers becomes large. However, the band at $\lambda = 530$ nm ascribed to the Au nanoparticles remains, which shows that some free Au nanoparticles still existed in solution when the polymerization reaction was completed. Therefore, the results of the UV-visible spectra not only confirm the formation of Au and polyaniline but also prove that the produced PANI evolves from oligomers. We have also investigated the doping/dedoping feature of Au/PANI-CSA nanocable films fabricated through in situ deposition from the reaction (inset in Figure 4). The Au/PANI-CSA nanocable film has an absorbance peak maximum at $\lambda = 420$ nm, which is ascribed to the polyaniline. The polaron band in the $\lambda = 650$ nm region confirms the presence of PANI in the conducting form (Figure 4d). As the film was dedoped with NH_4OH, the PANI peak at $\lambda = 420$ nm decreased and the polaron band at $\lambda = 650$ nm gradually disappeared. A strong absorption peak due to exciton transition of the quinoid ring appears at about $\lambda = 580$ nm, suggesting that the Au/PANI-CSA nanocables have been completely dedoped to the base form (Figure 4e). The Au/PANI-CSA nanocables returned to the conducting form when the film was redoped with HCl (Figure 4f). These results suggest that the polyaniline sheath in gold/polyaniline nanocables could still be doped and dedoped, which means that the gold/polyaniline nanocables can be further made into metal/insulator and metal/semiconductor core–sheath structures.

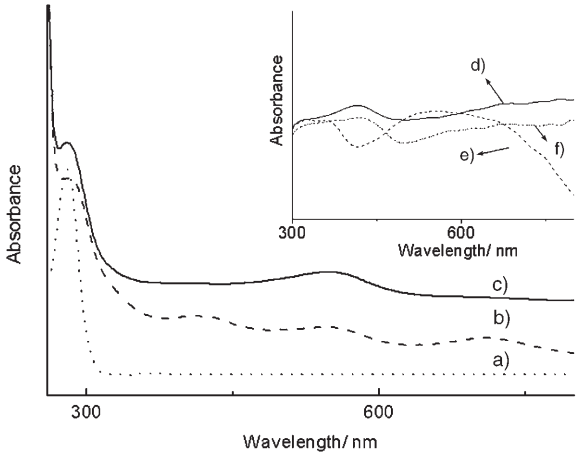

Figure 4. UV/Vis spectra of the chemically synthesized Au/PANI-CSA nanocables in aqueous solution under typical conditions with a reaction time of a) 0, b) 0.5, and c) 10 h. Inset: the UV/Vis spectra of the Au/PANI-CSA nanocable films fabricated by in situ deposition from the reaction under typical conditions, with the following NH_4OH/HCl dedoping/doping: d) Au/PANI-CSA nanocables film; e) dedoped with NH_4OH; f) redoped with HCl.

The molecular structure of the resulting Au/PANI-CSA nanocables was further characterized by FTIR spectroscopy and X-ray diffraction (XRD) measurements. The characteristic bands of PANI at wavenumbers of 1574 cm^{-1} (assigned to the C=C stretching of the quinoid rings), 1496 cm^{-1} (C=C stretching of benzenoid rings), 1306 cm^{-1} (C–N stretching mode), and 1143 cm^{-1} (N=Q=N, Q representing the quinoid ring) were observed clearly in the FTIR spectra of Au/PANI-CSA nanocables (Figure 5), and are identical to those of the emeraldine salt form of PANI reported earlier.[29] The presence of Au in the Au/PANI-CSA nanocables was further confirmed by a powder XRD pattern, as shown in Figure 6. Four strong bands appeared with maximum intensity at 38.1, 44.3, 64.5, and 77.5° representing Bragg reflections from the (111), (200), (220), and (311) planes of Au. The unit-cell constant a of such an *fcc* lattice was obtained

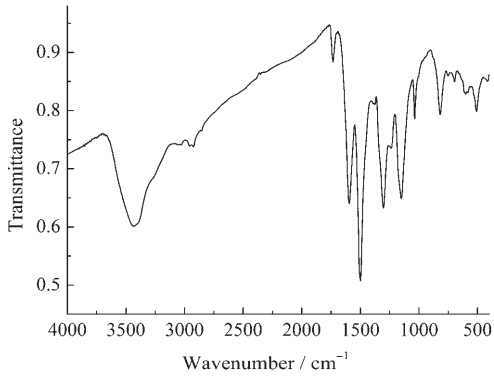

Figure 5. FTIR spectrum of the Au/PANI-CSA nanocables dispersed in a KBr pellet.

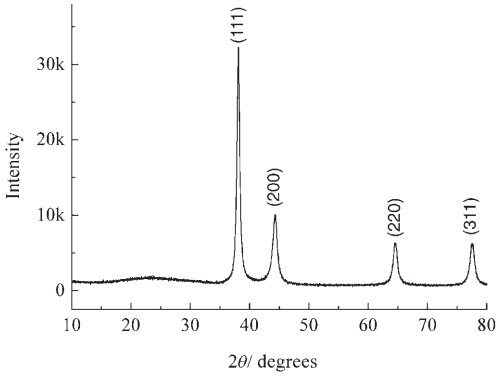

Figure 6. XRD pattern of the Au/PANI-CSA nanocables.

as 4.086 Å. A weak, broad peak centered at $2\theta = 23.3°$ may be attributed to the amorphous PANI-CSA.

Electrical properties of a single Au/PANI-CSA nanocable: A single Au/PANI-CSA nanocable with a length of 5 μm and an outer diameter of 180 nm was selected to investigate its electrical properties. Because the nanocable is not very long, only two platinum microleads were attached onto the single nanocable (it is difficult to fabricate four microleads of such a short length). Figure 7a shows a typical scanning electron microscopy (SEM) image of a single Au/PANI-CSA nanocable and the attached platinum microleads (length = 80 μm, cross section = $0.8 \times 0.4\ \mu m^2$). Because the resistivity of the platinum leads deposited by focused-ion-beam systems is about $5 \times 10^{-4}\ \Omega cm$,[30] the resistance of the platinum microleads can be estimated to be about 0.4 kΩ. Compared with the resistance of a single Au/PANI-CSA nanocable (20–200 kΩ), the resistance of the Pt electrodes is small.

Figure 7b shows the temperature (T) dependence of the resistance (R) of the single Au/PANI-CSA nanocable, whose resistance was measured by using a two-probe method. The single-nanocable conductivity (σ) can be determined by using Equation (1):

$$\sigma(T) = \frac{L}{SR(T)} = \frac{L}{\pi r^2 R(T)} \tag{1}$$

in which L is the length of the nanocable between two platinum microleads, S is the section area of a single nanocable, and r is the radius of the nanocable. We can deduce that the electrical conductivity of a single Au/PANI-CSA nanocable is $77.2\ S cm^{-1}$ at room temperature, which is much higher than the conductivity of a single PANI-CSA nanotube ($31.4\ S cm^{-1}$).[31,32] The Au/PANI-CSA nanocable shows semiconductive behavior. The resistivity increases with decreasing temperature, and $\sigma(100\ K) = 48.4\ S cm^{-1}$. It was found that the resistivity ratio of $\sigma_r = \sigma(100\ K)/\sigma(300\ K)$ is 1.6, which is much smaller than that of a single PANI-CSA nanotube ($\sigma_r = 7.4$).[31,32] The semiconducting behavior of conducting polymers can be described by the variable range hopping (VRH) model proposed by Mott and Davis[33] as

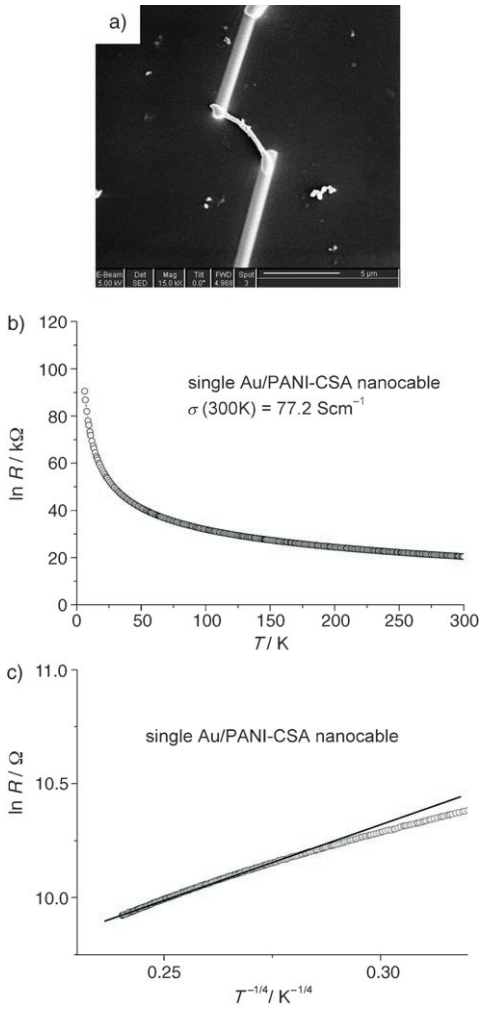

Figure 7. a) Typical SEM image of a single Au/PANI-CSA nanocable and Pt microelectrodes (scale bar = 5 μm). The length of the Pt microelectrode is 80 μm and its cross section is $0.8 \times 0.4\ \mu m^2$. b) Temperature dependence of the resistance of a single Au/PANI-CSA nanocable; the resistance is measured by a two-terminal technique; c) plot of $\ln R(T)$ versus $T^{-1/4}$ (R was measured in Ohms).

shown in Equations (2) and (3):

$$\sigma(T) = \sigma_0 \exp\left[\left(\frac{T_0}{T}\right)^{1/(n+1)}\right] \qquad (n = 1, 2, 3) \tag{2}$$

$$T_0 = \frac{8}{ZL_C N(E_F) k_B} \tag{3}$$

in which T_0 is the characteristic Mott temperature, which reflects the hopping energy, L_C is the localization length, $N(E_F)$ is the density of states at the Fermi level, k_B is the Boltzmann constant, Z is the number of nearest neighbor chains, and "$n = 1$, 2, and 3" means 1D, 2D, and 3D VRH conduction. Figure 7c shows the 3D-VRH plot of $\ln R(T)$ versus $T^{-1/4}$. The characteristic Mott temperature T_0 is about 260 K, which is also much smaller than that of a single PANI-CSA nanotube ($T_0 = 1500$ K).[29,30] The above results suggest that the Au nanowires in the Au/PANI-CSA nanoca-

ble can enhance the electrical properties of the Au/PANI-CSA composites. Such work is now in progress.

Conclusion

In conclusion, we have successfully developed a self-assembly method for synthesizing Au/PANI-CSA coaxial nanocables with average diameters of 50 nm and lengths of 1–2 μm in aqueous solution at low temperature. Dissolution of the Au nanowire core easily results in the formation of hollow PANI-CSA nanotubes. In this method, the aniline monomer was oxidized by $HAuCl_4$ in the presence of CSA (as the dopant and surfactant) leading to the formation of Au/PANI-CSA coaxial nanocables. The directly measured conductivity of a single gold/polyaniline nanocable is high ($\approx 77.2\ S\,cm^{-1}$). The synergistic effects of both growth of Au nanowires and the polymerization of PANI sheaths are responsible for the formation of the nanocables through a self-assembly process. Furthermore, we believe that the electronic interaction between the metal and the external conducting polymer layer will play a crucial role in constructing optoelectronic nanodevices.

Experimental Section

General: The aniline monomer (Aldrich, >99.5%) was distilled under reduced pressure and stored under N_2 gas. D-CSA (98%) and $HAuCl_4$ (>49%) were used as received (Aldrich).

Synthesis: In a typical experiment, the aniline monomer (16.5 μL) was mixed with an aqueous CSA solution (2.5 mL, 0.1 M) under stirring for 0.5 h to obtain a uniform emulsion. An aqueous solution of $HAuCl_4$ (0.5 mL, 50 mM) was quickly added to this emulsion. Then, the mixture was allowed to react at 0–5 °C (in an ice bath) for 10 h without stirring. The product was washed with deionized water several times, and finally dried under vacuum for 24 h to obtain a dark powder of Au/PANI-CSA nanocomposites.

Analysis: The electron microscopy of Au/PANI-CSA coaxial nanocables was carried out by using a transmission electron microscope (JEOL2000). UV/Vis absorption spectra of the reaction mixture at different reaction times in aqueous solution were recorded on a Shimadzu UV-3100 spectrometer. FTIR spectra (Perkin–Elmer system) and X-ray diffraction (MAC Science, Japan M-18AHF) analyses were used to characterize the molecular structure of Au/PANI-CSA nanocomposites.

Conductivity measurements: The platinum microleads were attached to the single nanocable as follows. First, some Au/PANI-CSA nanocables were ultrasonically dispersed in ethanol for about 15 min. Then, a drop of the dilute solution was placed on an insulating silica/Si substrate. Second, when the solution was dry, an electron microscope was used to find an appropriate single nanocable. Third, one pair of platinum microleads with a width of 0.8 μm and a thickness of 0.4 μm were fabricated by focused ion beam (FIB) deposition (Dual-Beam 235 FIB System from FEI Company). The electrical connection between the platinum microleads and the sample holder was made by using a highly conductive silver paste and gold wires. The electrical resistance of the single nanocable was measured by using a Physical Property Measurement System from Quantum Design.

Acknowledgements

The authors are most grateful to the NSFC, China (grant no. 20475053), and to the Department of Science and Technology of Jilin Province (grant no. 20050102) for financial support.

[1] L. J. Lauhon, M. S. Gudiksen, D. Wang, C. M. Lieber, *Nature* **2002**, *420*, 57–61.
[2] H. J. Choi, J. C. Johnson, R. He, S. K. Lee, F. Kim, P. Pauzauskie, J. Goldberg, R. J. Saykally, P. D. Yang, *J. Phys. Chem. B* **2003**, *107*, 8721–8725.
[3] S. O. Obare, N. R. Jana, C. J. Murphy, *Nano Lett.* **2001**, *1*, 601–603.
[4] Y. Yin, Y. Lu, Y. Sun, Y. Xia, *Nano Lett.* **2002**, *2*, 427–430.
[5] K. S. Mayya, D. I. Gittins, A. M. Dibaj, F. Caruso, *Nano Lett.* **2001**, *1*, 727–730.
[6] J. Cao, J. Z. Sun, J. Hong, H. Y. Li, H. Z. Chen, M. Wang, *Adv. Mater.* **2004**, *16*, 84–87.
[7] J. Jang, B. Lim, J. Lee, T. Hycon, *Chem. Commun.* **2001**, *1*, 83–84.
[8] M. Reches, E. Gazit, *Science* **2003**, *300*, 625–627.
[9] S. H. Yu, X. J. Cui, L. Li, K. Li, B. Yu, M. Antoniem, H. Colfen, *Adv. Mater.* **2004**, *16*, 1636–1640.
[10] L. B. Luo, S. H. Yu, H. S. Qian, T. Zhou, *J. Am. Chem. Soc.* **2005**, *127*, 2822–2823.
[11] W. Z. Li, S. S. Xie, L. X. Qian, B. H. Chang, B. S. Zhou, W. Y. Zhou, R. A. Zhao, G. Wang, *Science* **1996**, *274*, 1701–1703.
[12] E. Lindner, V. V. Cosofret, S. Ulfer, R. P. Buck, *J. Chem. Soc. Faraday Trans.* **1993**, *89*, 361–367.
[13] H. Sakai, R. Baba, K. Hashimoto, A. Fujishma, *J. Phys. Chem.* **1995**, *99*, 11896–11900.
[14] M. Trau, N. Yao, E. Kim, Y. Xia, G. M. Whitesides, I. A. Aksay, *Nature* **1997**, *390*, 674–676.
[15] J. H. Fendler, *Chem. Mater.* **1996**, *8*, 1616–1624.
[16] D. D. Lasic, *Liposomes. From Physics to Applications*, Plenum, New York, **1993**.
[17] J. M. Schnur, *Science* **1993**, *262*, 1669–1676.
[18] H. Q. Cao, Z. Xu, H. Sang, D. Sheng, C. Y. Tie, *Adv. Mater.* **2001**, *13*, 121–123.
[19] Y. J. Kim, J. H. Song, *Bull. Korean Chem. Soc.* **2005**, *26*, 227.
[20] J. X. Zhang, G. Q. Shi, C. Liu, L. T. Qu, M. X. Fu, F. E. Chen, *J. Mater. Sci.* **2003**, *38*, 2423.
[21] A. H. Chen, H. Q. Wang, X. Y. Li, *Chem. Commun.* **2005**, *14*, 1863–1864.
[22] R. J. Tseng, J. X. Huang, J. Y. Ouyang, R. B. Kaner, Y. Yang, *Nano Lett.* **2005**, *5*, 1077–1080.
[23] Z. X. Wei, Z. M. Zhang, M. X. Wan, *Langmuir* **2002**, *18*, 917–921.
[24] X. Sun, S. Dong, E. Wang, *Chem. Commun.* **2004**, 1182–1183.
[25] J. M. Kinyanjui, D. W. Hatchett, J. A. Smith, M. Josowicz, *Chem. Mater.* **2004**, *16*, 3390–3398.
[26] J. X. Huang, R. B. Kaner, *Angew. Chem.* **2004**, *116*, 5941–5945; *Angew. Chem. Int. Ed.* **2004**, *43*, 5817–5821.
[27] W. R. Salaneck, B. Liedberg, O. Inganäs, R. Erlandsson, I. Lundström, A. G. MacDiarmid, M. Halpern, N. L. D. Somasiri, *Mol. Cryst. Liq. Cryst.* **1985**, *121*, 191.
[28] A. N. Ship, M. Lahav, R. Gabai, T. Willner, *Langmuir* **2000**, *16*, 8789–8795.
[29] J. S. Tang, X. B. Jing, B. C. Wang, F. S. Wang, *Synth. Met.* **1988**, *24*, 231–238.
[30] J. F. Lin, J. P. Bird, L. Rotkina, P. A. Bennett, *Appl. Phys. Lett.* **2003**, *82*, 802–804.
[31] Y. Z. Long, Z. J. Chen, N. L. Wang, Y. J. Ma, Z. Zhang, L. J. Zhang, M. X. Wan, *Appl. Phys. Lett.* **2003**, *83*, 1863–1865.
[32] Y. Z. Long, L. J. Zhang, Z. J. Chen, K. Huang, Y. S. Yang, H. M. Xiao, M. X. Wan, A. Z. Jin, C. Z. Gu, *Phys. Rev. B* **2005**, *71*, 165412–165413.
[33] N. F. Mott, E. A. Davis, *Electronic Processes in Noncrystalline Materials*, Clarendon Press, Oxford, UK, **1979**.

Received: December 7, 2005
Revised: February 9, 2006
Published online: April 21, 2006

